JOURNAL OF MATERIALS SCIENCE 32 (1997) 4541–4547

Microwave-assisted oxygenation of melt-processed bulk $YBa_2Cu_3O_{7-\delta}$ ceramics

A. T. ROWLEY, R. WROE
EA Technology, Capenhurst, Chester CH1 6ES, UK

D. VÁZQUEZ-NAVARRO
Department of Materials Science and Metallurgy, University of Cambridge, Cambridge CB2 3QZ, UK

WAI LO, D. A. CARDWELL
IRC in Superconductivity, University of Cambridge, Madingley Road, Cambridge CB3 0HE, UK

The properties (superconducting and non-superconducting) of $YBa_2Cu_3O_{7-\delta}$ bulk ceramics (YBCO) are strongly dependent on the oxygen deficiency, δ. Unfortunately, whether sintering or melt-processing is used to form the material, the final oxygen content is usually far from that which gives the optimum superconducting properties ($\delta \lesssim 0.1$). Because of this, an additional oxygenation stage has to be carried out in which the material is heated and held at some elevated temperature ($\sim$400–500 °C) for a significant time (often $>$100 h) to allow oxygen to diffuse into the sample. Other diffusion-based processes (e.g. sintering) are known to be substantially enhanced in the presence of a microwave field, and it is reasonable to expect that the diffusion of oxygen into YBCO may also benefit from the application of such technology. The oxygenation of melt-processed YBCO using conventional and microwave-assisted heating has been compared. The diffusion coefficient at 400 and at 450 °C is shown to be enhanced by about 30% through the application of a high-frequency microwave field. Because the oxygenation time is inversely proportional to the diffusion coefficient, this represents a significant reduction in process time. The equilibrium value of the oxygen content is not affected by the application of a microwave field, and therefore the sample temperature must be the same for both microwave-assisted and conventional processing. Consequently, the observed enhancement is an example of a genuine non-thermal microwave effect.

1. Introduction

The electrical (superconducting and normal) and structural properties of high critical temperature, T_c, superconductors (HT_cS) are known to be dependent on their oxygen concentration. In the case of $YBa_2Cu_3O_{7-\delta}$ ceramics (YBCO), the properties are determined by the oxygen deficiency, δ. For example, T_c falls from $\sim$90 K when $\delta = 0.15$ to $T_c = 50$ K when $\delta = 0.5$, and eventually to zero when $\delta > 0.6$ [1]. The actual oxygen deficiency in YBCO is determined by the processing route and process conditions chosen.

Traditional ceramic processing of bulk YBCO relies on sintering to produce high-density samples comprised of a large number of small grains. Unfortunately, the boundaries between these grains represent weak links to the flow of super-currents, and YBCO samples processed in this way have relatively poor superconducting properties – even when the oxygen content is optimized. Typically, such material has a critical current density, J_c, of only about 1000 A cm^{-2} [2]. Because of this, a variety of melt-processing techniques have been developed to fabricate large-grain (YBCO) ceramics which have few or no grain boundaries, and which exhibit critical currents of up to $\sim 5 \times 10^4$ A cm^{-2} at 77 K and 1 T [3–9]. Whether sintering or melt-processing is used to manufacture YBCO components, the oxygen content at the end of these processes is often far from the optimum, and an additional oxygenation (or annealing) stage has to be carried out.

The best melt-processed $YBa_2Cu_3O_{7-\delta}$ (often denoted as the Y-123 phase) also contains a fine dispersion of Y_2BaCuO_5 (Y-211 phase) embedded within the Y-123 matrix, which is not present in the sintered material. All melt-processing techniques used to fabricate large-grain YBCO ceramics exploit a peritectic reaction at about 1015 °C where the 123 phase is formed from the 211 phase and a liquid phase with the stoichiometry $Ba_3Cu_5O_{6.72}$ [7], i.e.

$$Y_2BaCuO_5(s) + Ba_3Cu_5O_{6.72}(l) + 0.42O_2(g) \rightarrow 2YBa_2Cu_3O_{6.28}(s) \quad (1)$$

0022–2461

The Y-211 phase and the liquid in this reaction can be produced by rapidly heating a pre-sintered green body of the desired composition to a temperature well above the peritectic temperature, T_p. Formation of the required Y-123 phase is then achieved by slowly cooling (at about 1–2 °C h^{-1}) the partially molten YBCO material back through T_p. Typically, samples are cooled in this way to around 900 °C, and then further cooled relatively quickly back to room temperature.

At the end of this process, the oxygen content will still be close to 6.3 (i.e. $\delta = 0.7$) – at which level YBCO superconducts only at low temperatures, and an additional processing stage is carried out to increase the oxygen content towards $\delta \lesssim 0.1$ (highest T_c values). A typical oxygenation process involves heating the melt-processed sample to around 400–500 °C and holding it at that temperature for several tens of hours. During this time, oxygen from the surrounding atmosphere diffuses into the sample, reducing the oxygen deficiency. The equilibrium value of δ reached in this way depends on the temperature and the partial pressure of oxygen surrounding the sample [10, 11]. The smallest values of δ ($\sim$0.05) are obtained at high oxygen partial pressures and at low temperatures (< 300 °C) – the variation of δ with temperature in air ($P(O_2) = 0.2$ atm) is shown in Fig. 1. Unfortunately, at the low temperatures required to achieve small values of δ, the diffusion coefficient for the movement of oxygen through the $YBa_2Cu_3O_{7-\delta}$ is very small, and higher temperatures have to be used to limit the total oxygenation time to a manageable value. If the diffusion of oxygen could be enhanced in some way (e.g. through a higher effective diffusion constant) it will become possible to reduce these oxygenation times. Alternatively, a higher oxygen content could be achieved with the same processing time.

There is now a growing amount of experimental evidence to support the fact that microwave heating of ionic crystalline solids leads to an enhancement of the diffusion processes which occur during the sintering in these materials (see [12] for a review of microwave processing). Samples processed within a microwave furnace are observed to sinter at a faster rate or at a lower temperature than those processed in a conventional system. For example, Wilson and Kunz [13] demonstrated that partially stabilized zirconia (with 3 mol % yttria) could be rapidly sintered using 2.45 GHz microwaves with no significant difference in the final grain size. The sintering time was reduced from 2 h to about 10 min. Many authors have incorporated this enhancement into the conventional theories of sintering through the introduction of an effective activation energy for the diffusion processes taking place during sintering (increasing the vacancy mobility through the lattice). Most notably, Janney *et al.* [14, 15] have shown that, at 28 GHz, the microwave-enhanced densification of high-purity alumina proceeds as if the activation energy is reduced from 575 kJ mol^{-1} to 160 kJ mol^{-1}.

Despite the potential implication for the ceramics industry, there has been little work published which discusses the possible physical mechanisms for such a large reduction in activation energy. The microwaves must interact with the ceramic in order to reduce the actual activation energy or to increase the effective driving force experienced by the diffusing species. Bookse *et al.* [16] suggested that the microwaves interact with the crystal lattice in such a way as to render the Boltzmann approximation used in the derivation of the diffusion coefficient, invalid. However, in later calculations, by the same group, Freeman *et al.* [17] indicated that extremely high microwave electric field strengths would be required for this to occur ($\sim 10^7$ V m^{-1}) – much higher than typical field strengths in a microwave applicator ($\sim 10^3$–10^4 V m^{-1}). In the same paper, Freeman *et al.* published results of conductivity measurements made on a single crystal of NaCl which indicated that the vacancy mobility is not enhanced by the application of microwaves, but that the diffusion driving force is enhanced. Further evidence for the existence of an enhancement to the driving force was also presented in a recent paper by Wroe and Rowley [18]. These results are consistent with the calculations of Rybakov and Semenov [19] who show that the driving forces for vacancy motion can be enhanced near a surface or boundary.

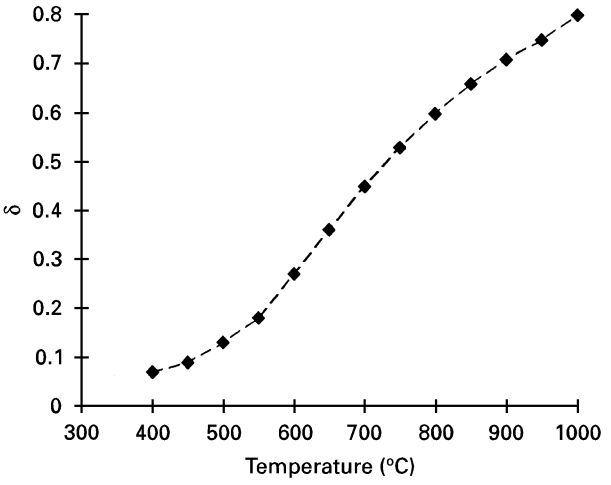

Figure 1 Variation of oxygen deficiency, δ, in $YBa_2Cu_3O_{7-\delta}$ as a function of temperature (from [10]).

Like the oxygenation of high-temperature superconductors, the thermal sintering of ceramics is a diffusion-based process, and it is reasonable to expect that the same microwave-induced enhancement experienced in sintering may also be possible in the case of superconductors. The purpose of this work was to determine if any such enhancement is present in the oxygenation of melt-processed YBCO in the presence of a microwave field. In this work, the change in the weight of the sample will be used to follow the oxygenation process – both with and without the application of a high-frequency microwave field.

2. Theory

2.1. Oxygen diffusion and oxygenation

The diffusion processes taking place during sintering and the diffusion of oxygen through melt-processed

YBCO are both described by Fick's law (e.g. [20])

$$\boldsymbol{J} = -D\,\mathrm{grad}(C) \tag{2}$$

In this equation, $\boldsymbol{J}$ is the net oxygen atom flux, C is the local oxygen concentration, and D is the diffusion coefficient for this process given by

$$D = D_0 e^{-\frac{E_a}{kT}} \tag{3}$$

where, D_0 is a constant (the pre-exponential factor), k is Boltzmann's constant, T is the absolute temperature, and E_a is the activation energy for the diffusion process. The oxygen flux, represented by Fick's law, can be thought to be the product of a mobility term, D, and a driving force term (the concentration gradient). If either term is increased, then the diffusion will be enhanced.

Setting the change in concentration with time $(\delta C/\delta t)$ equal to $-\mathrm{grad}(\boldsymbol{J})$ and substituting for $\boldsymbol{J}$ using Equation 2, produces Fick's second equation. In one dimension, if the diffusion coefficient is independent of concentration, this simplifies to

$$\frac{\partial C(x,t)}{\partial t} = D\,\frac{\partial^2 C(x,t)}{\partial x^2} \tag{4}$$

Solutions to this differential equation give the variation of oxygen content with position and time, $C(x,t)$. Actual solutions to Equation 4 depend on the boundary conditions of any given problem. This equation is exactly analogous to the one-dimensional heat-flow equation, and solutions for many boundary conditions and geometries are given in a large number of applied mathematics and physics texts (e.g. [21]).

2.1.1. Absorption of oxygen (weight gain)

For oxygen diffusing into a sample of thickness $2h$, with an initial oxygen content of C_0, $C(x,t)$ is given by

$$\frac{C(x,t) - C_o}{C_f - C_o} = 1 - \frac{4}{\pi}\sum_{n=0}^{\infty}\frac{(-1)^n}{2n+1} \times \exp\left[-(2n+1)^2\,\frac{\pi^2}{4}\,\frac{Dt}{x^2}\right] \times \cos\left(\frac{2n+1}{2}\,\pi\,\frac{x}{h}\right) \tag{5}$$

where C_f is the equilibrium oxygen content reached after an infinite amount of time has passed [22]. The variation of the distribution of oxygen concentration, $C(x)$, at a number of times for a material with a thickness of 1 cm and a diffusion coefficient of $5\times10^{-10}\,\mathrm{m^2\,s^{-1}}$ is shown in Fig. 2. In this example, the equilibrium oxygen content is reached after approximately 20 h.

Integrating Equation 5 gives the variation of total oxygen content with time, and hence the variation of sample weight with time, $M(t)$, can be written

$$\frac{M(t) - M_o}{M_f - M_o} = 1 - \frac{8}{\pi^2}\sum_{n=0}^{\infty}\frac{1}{(2n+1)^2} \times \exp\left[-(2n+1)^2\,\frac{\pi^2}{4}\,\frac{Dt}{h^2}\right] \tag{6}$$

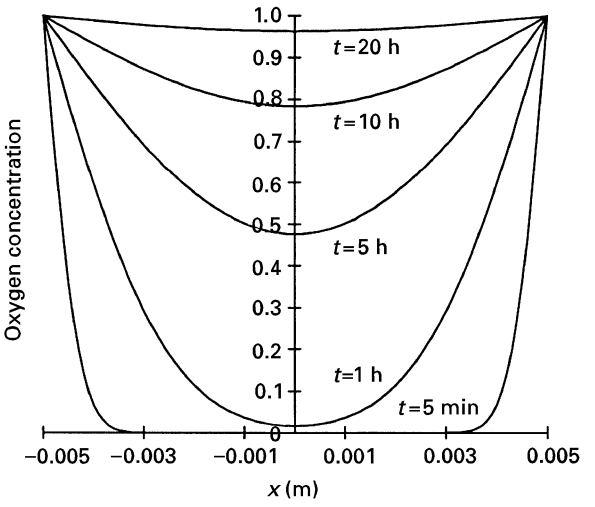

Figure 2 Theoretical variation of oxygen content with the position in the sample for oxygenation for different times (from Equation 5). $D_{eff} = 5\times10^{-10}\,\mathrm{m^2\,s^{-1}}$ and sample thickness = 1.0 cm.

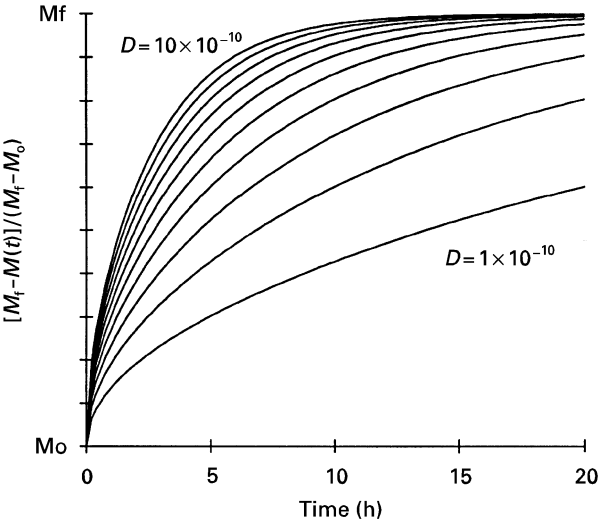

Figure 3 Theoretical variation of sample weight with time during oxygenation for different diffusion coefficients (from Equation 7). Sample thickness = 1.0 cm.

Apart from at short times, only the first term of this sum is significant and, following some re-arrangement, this function reduces to

$$\frac{M_f - M(t)}{M_f - M_o} = \frac{8}{\pi^2}\exp\left(-\frac{\pi^2}{4}\,\frac{Dt}{h^2}\right) \tag{7}$$

Fig. 3 shows the variation of the total amount of oxygen with time for a range of diffusion coefficients between $10^{-10}\,\mathrm{m^2\,s^{-1}}$ and $10^{-9}\,\mathrm{m^2\,s^{-1}}$ for a 1 cm thick sample. Clearly, the shape of the curve changes with diffusion coefficient. For a given oxygenation process, the shape of this curve will then give an approximate value for D and, providing the process time is long enough (i.e. $t \gtrsim (4h^2/\pi^2 D)$), a value for M_f. More accurately, a graph of $\ln[M_f - M(t)/(M_f - M_o)^{-1}]$ versus time should be a straight line with gradient equal to $-(\pi^2 D/4h^2)$, and an intercept at $\ln(8/\pi^2)$ i.e. -0.210.

2.1.2. Desorption of oxygen (weight loss)

When the oxygen content within the sample is greater than the equilibrium value, the solution of Equation 4 for out-diffusion of oxygen is given by the sum of two error functions [21]

$$\frac{C(x,t) - C_f}{C_o - C_f} = \frac{1}{2}\left\{\mathrm{erf}\left[\frac{h + x}{2(Dt)^{1/2}}\right] + \mathrm{erf}\left[\frac{h - x}{2(Dt)^{1/2}}\right]\right\} \quad (8)$$

Integrating Equation 8 over the thickness of the sample, $2h$, gives the total amount of oxygen desorbed by the sample as a function of time. Hence the weight of the sample during desorption of oxygen is given by

$$\frac{M(t) - M_f}{M_o - M_f} = \int_{-h}^{h} \frac{1}{2}\left\{\mathrm{erf}\left[\frac{h + x}{2(Dt)^{1/2}}\right] + \mathrm{erf}\left[\frac{h - x}{2(Dt)^{1/2}}\right]\right\} dx \quad (9)$$

3. Experimental procedure

3.1. Sample preparation

The bulk YBCO ceramics used in these experiments were prepared using the seeded melt-growth (SMG) technique initially developed by Sawano *et al.* [23]. Using this technique, the nucleation of the Y-123 phase in these samples is controlled by a small (RE) $Ba_2Cu_3O_{7-\delta}$ (RE = rare-earth) single-crystal seed placed on the top of a pre-sintered YBCO specimen prior to melt processing.

Precursor powders containing fine Y-123 and Y-211 particles were prepared by spray-drying and then calcining a nitrate solution containing yttrium, barium and copper cations in the right proportion to give a final composition of $YBa_2Cu_3O_{7-\delta} + 0.3Y_2BaCuO_5$ [24, 25]. The YBCO pellets used for the SMG processing were formed by compressing this powder in a uniaxial die followed by sintering for 8 h at 930 °C, producing pellets with a density of about 5.5 g cm^{-3} [26].

After positioning a small ($\sim$1 mm^3) $SmBa_2Cu_3O_{7-\delta}$ seed crystal in the centre of the pellets, the samples were heated at 10 °C h^{-1} to 1100 °C (above the peritectic melting point) and then cooled slowly at 2 °C h^{-1} through the peritectic transition temperature to 910 °C to form the Y-123 phase. The furnace used for this stage of the process was specially designed to allow the cooling to take place in precisely controlled horizontal and vertical temperature gradients, thus ensuring that large grains of the Y-123 phase were obtained [7]. Finally, the samples were cooled at approximately 10 °C min^{-1} back to room temperature. The resultant bulk YBCO ceramic samples produced in this way are cylindrical discs with a diameter of 3 cm and a thickness of 0.7 cm.

3.2. Measurement procedure

These oxygenation experiments were carried out in a furnace specially designed to allow microwave and conventional heating sources to operate simultaneously [27]. The system, shown schematically in Fig. 4, is essentially a conventional furnace built within a multi-mode 2.45 GHz microwave cavity powered by a 1.2 kW industrial-standard magnetron. Care has been taken in the design and construction of the radiant heating elements to avoid any unwanted interaction between the two heating sources. For example, the radiant heating elements could severely affect the distribution of the high-frequency fields within the cavity.

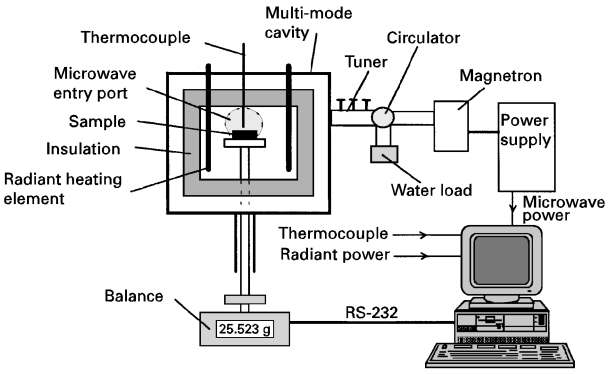

Figure 4 Measurement apparatus for microwave-assisted oxygenation experiments.

The thermocouple used in the furnace is encased in a metal sheath, and is positioned to minimize its effect on the microwave field distribution. In these experiments the thermocouple is used to control the power to the radiant heating elements; the amount of microwave power is set manually.

The melt-processed YBCO sample is mounted on an alumina platform positioned approximately in the centre of the furnace, and supported by an alumina tube attached to the weighing pan of a Mettler PM2000 balance ($\pm$0.001 g). The sample weight, temperature, radiant and microwave powers are continuously monitored and recorded by a personal computer. All experiments reported here were carried out with air surrounding the sample.

In essence, there are two stages to the oxygenation experiments, corresponding to the absorption and desorption of oxygen from the sample. Because the equilibrium oxygen content (i.e. δ) is a function of temperature (Fig. 1), this corresponds to maintaining the sample at two different temperatures. The oxygenation process is reversible and the same sample can be used for the conventional and the microwave-assisted experiments. A typical experiment comprises of the following temperature/time schedule:

(i) ramp at 5 °C min^{-1} to 400 °C, hold for 20 h,
(ii) ramp at 5 °C min^{-1} to 750 °C, hold for 5 h,
(iii) ramp at 5 °C min^{-1} to 20 °C.

The shorter hold period at 750 °C reflects the larger diffusion coefficient at this temperature. Repeating this schedule with and without the application of microwaves during the 400 °C hold period allows the effect of microwaves on the oxygenation of YBCO to be determined.

For all the experiments reported here, the microwave power was set to between 900 and 1000 W. To some extent this is arbitrary, and does not reflect the amount of power absorbed by the sample. Because the

size of the sample is very small compared with the size of the furnace, most of the microwave power will be dissipated in the furnace insulation and cavity walls. In order to keep the sample temperature constant when the microwaves are applied, the radiant power is automatically reduced slightly (by the temperature controller).

4. Results and discussion

The complete variation of sample weight and temperature with time for a typical experiment is shown in Fig. 5. In essence, the sample is gaining weight (i.e. absorbing oxygen) during the hold period at 400 °C, and losing weight (desorbing oxygen) at 750 °C. Fig. 6 shows the same data but with the sample weight plotted against temperature rather than time. In this representation, the weight gain at 400 °C and the weight loss at 750 °C are clearly shown. However, the weight loss during the heating period from 400–750 °C and the weight gain during the cooling period from 750 °C are also of interest. The shape of the curves in these two regions, demonstrate that the rate of weight gain or weight loss (and so the diffusion coefficient) is a strong function of temperature – the rate of weight change increasing towards higher temperatures.

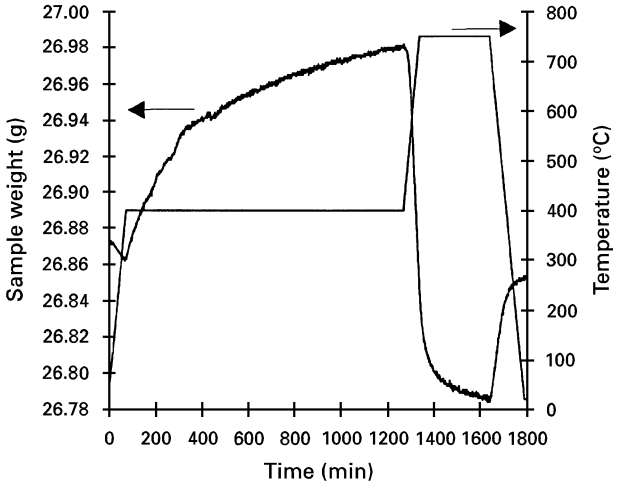

Figure 5 Microwave-assisted oxygenation of YBCO; 20 h hold at 400 °C followed by a 5 h hold at 750 °C.

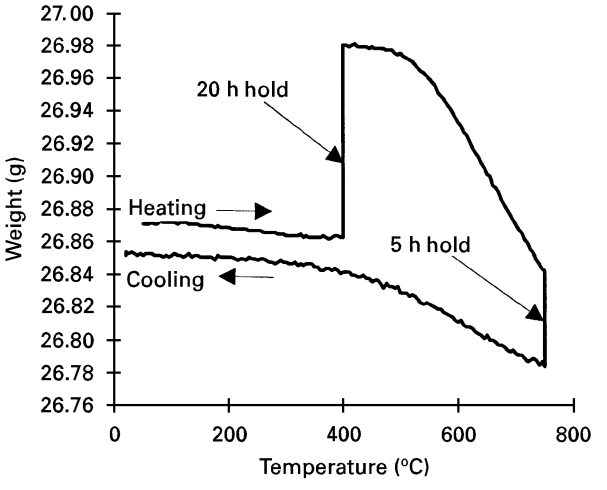

Figure 6 Change in sample weight with temperature for the microwave-assisted oxygenation of YBCO; 20 h hold at 400 °C followed by a 5 h hold at 750 °C.

4.1. Absorption of oxygen

The logarithmic sample weight variation with time at 400 °C for conventional and microwave-assisted processing is compared in Fig. 7. The dashed lines are best straight line fits to the data (from Equation 6). In these results, the equilibrium value of sample weight is taken to be 26.994 ± 0.002 g for conventional processing, and 26.990 ± 0.002 g for microwave-assisted processing. The gradients of the two lines give rise to effective diffusion coefficients of $1.22 \times 10^{-10}\ m^2\ s^{-1}$, and $1.64 \times 10^{-10}\ m^2\ s^{-1}$ for the conventional and the microwave-assisted experiments, respectively. The intercepts with the y-axis are -0.175 and -0.258, reasonably close to the expected value of $-0.210[\ln(8/\pi^2)]$.

To compare these results with those made at another temperature, a second pair of experiments were carried out on the same sample. In these experiments, the first hold period was for 10 h at 450 °C, otherwise the heating and cooling schedule was the same. Fig. 8 compares the results for the conventional and microwave-assisted experiments. At this temperature, the equilibrium sample weight is 26.960 ± 0.002 g for conventional processing and 26.965 ± 0.002 g for microwave-assisted processing. The gradients give corresponding effective diffusion coefficients of $1.79 \times 10^{-10}\ m^2\ s^{-1}$ and $2.33 \times 10^{-10}\ m^2\ s^{-1}$, respectively. (The y-axis intercepts are -0.205 and -0.183.)

The uncertainty in the calculated diffusion coefficients is about $\pm 5\%$. Both at 400 and at 450 °C, the microwave-assisted results give rise to a higher value

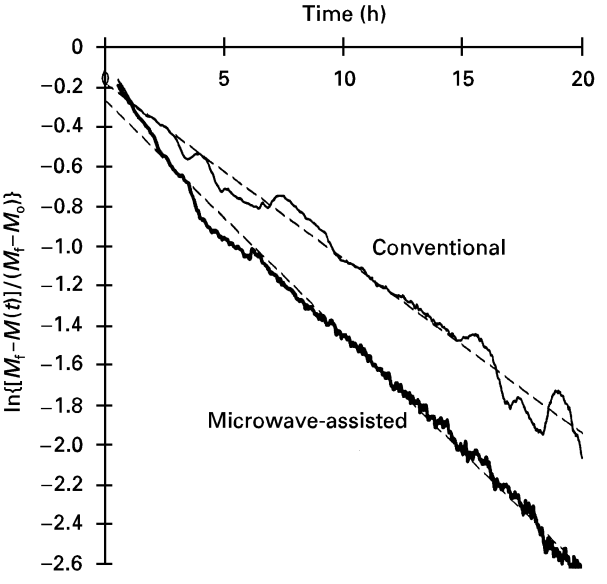

Figure 7 Comparison of conventional and microwave-assisted oxygenation of melt-processed YBCO; 20 h hold at 400 °C. Fit with $M_f = 26.994$ g (conventional) and $M_f = 26.990$ g (microwave-assisted). The gradient of the lines gives $D_{eff} = 1.22 \times 10^{-10}\ m^2\ s^{-1}$ with conventional heating and $D_{eff} = 1.64 \times 10^{-10}\ m^2\ s^{-1}$ with the microwave-assisted case.

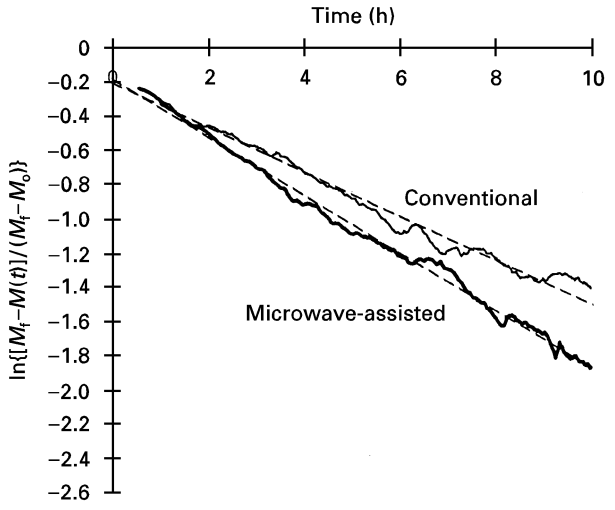

Figure 8 Comparison of conventional and microwave-assisted oxygenation of melt-processed YBCO; 10 h hold at 450 °C. Fit with $M_f = 26.960$ g (conventional) and $M_f = 26.965$ g (microwave-assisted). The gradient of the lines gives $D_{eff} = 1.79 \times 10^{-10}$ m^2 s^{-1} with conventional heating and $D_{eff} = 2.33 \times 10^{-10}$ m^2 s^{-1} with the microwave-assisted case.

of D_{eff} than the conventional results. The equilibrium sample weights are, within experimental accuracy, independent of processing route. At 400 °C, D_{eff} in the presence of microwaves is 28% (range 22%–48%) higher than that without microwaves. At 450 °C, D_{eff} is 30% (range 18%–44%) higher with the application of microwaves.

The effective diffusion coefficients observed here are considerably larger than those obtained from the literature which typically range from about 10^{-12}–10^{-15} m^2 s^{-1} at 400 °C [28–30] (compared with the $\sim 2 \times 10^{-10}$ m^2 s^{-1} measured here). The time constant, τ, for the diffusion process is given by $\tau = 4h^2/\pi^2 D_{eff}$, which, for a 7 mm thick sample is $\sim$7 h for $D_{eff} = 2 \times 10^{-10}$ m^2 s^{-1}; $\sim$1400 h for $D_{eff} = 10^{-12}$ m^2 s^{-1}; and 1.4×10^6 h for $D_{eff} = 10^{-15}$ m^2 s^{-1}. Because the oxygenation process is nearing completion after only 20 h at 400 °C, the measured effective (or apparent) diffusion coefficient must be approximately correct. The diffusion coefficients reported in the literature refer to those in single-crystal or high-density polycrystalline Y-123 material without the Y-211 inclusions, which are normally present in melt-processed YBCO grains. In these melt-processed samples, which are not fully dense, it is likely that oxygen diffuses rapidly into the pores in the sample and along the boundaries between the Y-123 and Y-211 phases. It then slowly diffuses through the bulk of the material – in effect the length scale is now much less than 7 mm, and the actual diffusion coefficient will be much higher. However, as far as process times are concerned, it is the apparent diffusion coefficient which is important.

One possible explanation of an increased value of the apparent diffusion coefficient with the application of microwaves is simply that the temperature is measured incorrectly in the presence of a microwave field (e.g. through the thermocouple interacting with the high-frequency electric field). However, the equilibrium value of oxygen deficiency, δ, is known to be highly temperature dependent (Fig. 1) and, since M_f (proportional to δ) is approximately the same with and without the application of microwaves, the sample temperature must also be the same. Therefore, the increase in the diffusion coefficients is a genuine non-thermal microwave effect. The mechanism by which the microwave field leads to enhanced oxygen diffusion cannot be elucidated from these results. Either the actual diffusion coefficient is increased, or the microwave field leads to the presence of an additional driving force term.

4.2. Desorption of oxygen

In these trials, only conventional desorption of oxygen was studied (the microwaves were only applied during the low-temperature hold period). Indeed, the hold at the higher temperature was only used to remove oxygen from the sample allowing the same sample to be used for a number of oxygenation experiments. Nevertheless, the results at this temperature can be used to obtain a value for the equilibrium oxygen content and the effective out-diffusion coefficient at this temperature. Fig. 9 shows the weight loss during desorption of oxygen at 750 °C. The solid line is a fit of Equation 9 to these data, and corresponds to $D_{eff} = 4.5 \times 10^{-9}$ m^2 s^{-1} and $M_f = 26.771$ g. In this example, the uncertainty in D_{eff} is about $\pm 10\%$ and the uncertainty in M_f is approximately ± 0.002 g.

4.3. Oxygen deficiency, δ

At the end of these experiments, the sample was placed in a conventional furnace for 72 h at 350 °C followed by 168 h at 300 °C in an attempt to reach the maximum oxygen content for oxygenation in air. The final sample weight was 27.040 g. Assuming that this corresponds to a δ of 0.05 and that the YBCO sample comprises the Y-123 phase mixed with a 30% molar excess of the Y-211 phase, this implies that the $\delta = 1.00$ weight would be 26.528 g. Consequently,

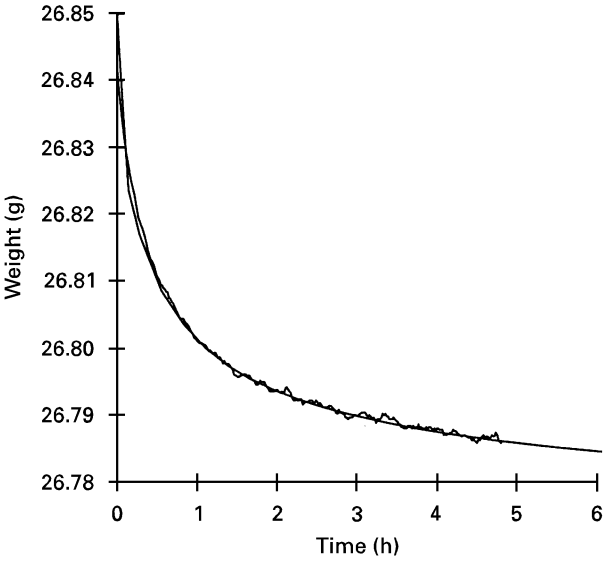

Figure 9 Weight loss during conventional desorption of oxygen from YBCO; 5 h hold at 750 °C. Fit with $M_o = 26.85$ g, $M_f = 26.771$ g and $D_{eff} = 4.5 \times 10^{-9}$ m^2 s^{-1}.

26.771 g at 750 °C is equivalent to $\delta = 0.55$; 26.962_5 g at 450 °C is equivalent to $\delta = 0.19$, and 26.992 g at 400 °C is equivalent to $\delta = 0.14$.

5. Conclusion

The use of microwaves in the oxygenation of melt-processed bulk YBCO ceramics leads to approximately a 30% increase in the effective, or apparent, diffusion coefficient. Because the oxygenation time is inversely proportional to the diffusion coefficient, this enhancement will lead to a 30% reduction in the total process time. Alternatively, in a given processing time, microwave-assisted oxygenation will lead to a higher oxygen content and, therefore, to improved superconducting properties. Moreover, the volumetric nature of microwave-assisted processing should give rise to material with a more uniform oxygen distribution, particularly when large samples are considered.

The equilibrium oxygen content is a strong function of processing temperature and, because this content is not affected by the use of microwave-assisted processing, the sample temperature must be the same whatever the processing route. Consequently, the enhancement of the effective diffusion coefficient is a genuine non-thermal microwave effect – even if conventional heating could be applied in the same volumetric way as microwave-assisted heating, this enhancement would not be observed.

Acknowledgements

This work has been undertaken by EA Technology through its Core Research programme on behalf of its members. The authors would like to thank the Directors of EA Technology for permission to publish it here. The receipt of a grant from the Department of Trade and Industry through its LINK Enhanced Engineering Materials Programme is gratefully acknowledged. The authors would also like to thank staff at the Interdisciplinary Research Centre in Superconductivity, Cambridge University, for useful discussions relating to this work, and the Croucher Foundation for their support of research at this establishment.

References

1. R. J. CAVA *et al.*, *Phys. C* **165** (1990) 419.
2. A. R. JONES, R. A. DOYLE, F. J. BLUNT and A. M. CAMPBELL, *Phys. C* **196** (1992) 63.
3. M. MURAKAMI, *Supercond. Sci. Technol.* **5** (1992) 185.
4. M. MORITA, V. SELVAMANICKAM and D. F. LEE, in "Processing and Properties of High T_c Superconductors, 1: Bulk Materials", edited by S. Jin (World Scientific, Singapore, 1993) pp. 155–212.
5. M. MORITA, S. TAKEBAYASHI, M. TANAKA, K. KIMURA, K. MIYAMOTO and K. SAWANO, in "Advances in Superconductivity III", Proceedings of the 3rd International Symposium Supplement, Sendai, November (1990) edited by K. Kajimura and H. Hayakawa (Springer-Verlag, Tokyo, 1991) pp. 733–6.
6. M. MURAKAMI, M. MORITA, K. DOI and K. MIYAMOTO, *Jpn J. Appl. Phys.* **28** (1989) 1189.
7. W. LO, D. A. CARDWELL, C. D. DEWHURST and S. L. DUNG, *J. Mater. Res.* **11** (1996) 786.
8. C. D. DEWHURST, W. LO and D. A. CARDWELL, *IEEE Trans. Appl. Supercond.*, submitted.
9. W. LO, D. A. CARDWELL and S. L. DUNG, *J. Mater. Res.* **11** (1996) 786.
10. K. KISHIO, J. SHIMOYAMA, T. HASEGAWA, K. KITAZAWA and K. FUEKI, *Jpn J. Appl. Phys.* **7** (1987) L1228.
11. W. LO, T. B. TANG, C. LI and Y. XU, *Appl. Phys. Lett.* **53** (1988) 2710.
12. W. H. SUTTON, *Ceram. Bull.* **68** (1989) 376.
13. J. WILSON and S. M. KUNZ, *J. Am. Ceram. Soc.* **71** (1988) c40.
14. M. A. JANNEY and H. D. KIMREY, *Mater. Res. Symp. Proc.* **189** (1991).
15. M. A. JANNEY, H. D. KIMREY, M. A. SCHMIDT and J. O. KIGGANS, *J. Am. Ceram. Soc.* **74** (1991) 1675.
16. J. H. BOOKSE, R. F. COOPER, I. DOBSON and L. McCAUGHN, in Ceramics Transactions, Vol. 21, "Microwaves: Theory and Application in Material Processing" edited by D. E. Clarke, F. D. Gac and W. H. Sutton (American Ceramic Society, Westerville OH, 1991) pp. 185–92.
17. S. FREEMAN, J. BOOKSE, R. COOPER and B. MENG, *Mater. Res. Symp. Proc.* **347** (1994) 479.
18. F. C. R. WROE and A. T. ROWLEY, *J. Mater. Sci.* **31** (1996) 2019.
19. K. I. RYBAKOV and V. E. SEMENOV, *Phys. Rev. B* **49** (1994) 64.
20. C. KITTEL, "Introduction to Solid State Physics" (Wiley, New York, 1976).
21. E. KREYSZIG, "Advanced Engineering Mathematics" (Wiley, New York, 1979).
22. H. SCHMALZRIED, "Solid state reactions", 2nd Edn. Monographs in Modern Chemistry (Verlag Chemie, 1981).
23. K. SAWANO, M. MORITA, M. TANAKA, K. SASAKI, K. KIMURA, S. TAKEBAYASHI, M. KIMURA and K. MIYAMOTO, *Jpn J. Appl. Phys.* **30** (1991) L1157.
24. W. LO, D. A. CARDWELL, S.-L. DUNG and R. G. BARTER, *IEEE Trans. Appl. Supercond.* **5** (1995) 1619.
25. *Idem*, *J. Mater. Res.* **11** (1996) 39.
26. *Idem*, *J. Mater. Sci.* **30** (1995) 3995.
27. EA Technology Ltd, International Pat. Appl. PCT/GB94/01730 (1993).
28. T. UMEMURA, K. EGAWA, M. WAKATA and K. YOSHIZAKI, *Jpn J. Appl. Phys.* **28** (1989) L1945.
29. A. P. MOZHAEV, S. V. CHERNYAEV, T. I. UDAL'TSOVA and N. M. KOTOV, *Russ. J. Inorg. Chem.* **37** (1992) 1111.
30. B. A. GLOWACKI, R. K. HIGHMORE, K. F. PETERS, A. L. GREER and J. E. EVETTS, *Supercond. Sci. Technol.* **1** (1988) 7.

Received 10 October 1996
and accepted 10 March 1997